Modeling, Identification and Control, Vol. 46, No. 1, 2025, pp. 35–49, ISSN 1890–1328

Modeling and Analyzing the Impact of Environmental Disturbances in Vessel Model Estimation

B. Sanguino T. Wang G. Li Ø.K. Kjerstad H. Zhang

Department of Ocean Operations and Civil Engineering, Norwegian University of Science and Technology, N-6009 Ålesund, Norway. E-mail: {beatriz.i.s.c.d.c.sanguino, tongtong.wang, guoyuan.li, oivind.k.kjerstad, hozh}@ntnu.no

Abstract

Environmental disturbances such as wind, currents, and waves introduce uncertainties in hydrodynamic parameter estimation, affecting the accuracy of ship maneuvering models and trajectory prediction. This study investigates how these disturbances influence the estimation of hydrodynamic derivatives in the Abkowitz maneuvering model and their impact on their accuracy. Therefore, models are estimated using least squares regression based on data from four maneuvers conducted under different wind and current conditions. A comparison of the resulting hydrodynamic derivatives identifies parameters that exhibit greater variance as disturbance intensity increases. To further assess their influence on the trajectory prediction error, Sobol sensitivity analysis is applied to determine which parameter variations most significantly affect trajectory accuracy. The results reveal that while some parameters remain stable across environmental conditions, others exhibit slight variations. Additionally, the parameters most affected by disturbances are not necessarily those with the greatest impact on trajectory prediction error. These findings highlight the importance of accounting for environmental effects in vessel model estimation to improve prediction reliability and provide deeper insight into how disturbances impact the model estimation process.

Keywords: Maneuvering Model; External disturbances; Parameter Estimation; Least Square Regression; Sensitivity Analysis

1 Introduction

Accurate vessel modeling is essential for safe navigation, efficient route planning, and the development of autonomous maritime systems. Several models have been proposed in the literature to describe the maneuvering dynamics of a vessel (Xu and Soares, 2025), including the Maneuvering Mathematical Group (MMG) model and the Abkowitz model. The Abkowitz model, based on a Taylor series expansion, is commonly used when maneuvering data, either from experimental trials (Xu et al., 2020; Yang and el Moctar, 2024) or simulations (Wang et al., 2020; Du et al., 2022), is available. This is due to the fact that the model's parameters, called hydrodynamic derivatives, can be estimated using regression techniques.

However, when collecting maneuvering data, external disturbances such as wind, currents, and waves inevitably affect measurements. These disturbances not only introduce uncertainty into the estimation process but can also lead to systematic biases, potentially resulting in inaccuracies in the identified parameters and, consequently, in trajectory predictions. Given the increasing reliance on model-based control and decision-making in modern maritime operations, understanding how environmental disturbances influence parame-

doi:10.4173/mic.2025.1.3

ter estimation is crucial for enhancing the reliability of ship models in practical applications.

Most studies on system identification for ship modeling assume controlled conditions or minimal external influences. However, in real-world scenarios, disturbances such as wind, waves, and currents are inevitable Xu and Soares (2025). These effects can lead to significant variations in parameter estimates, raising questions about the robustness of the models and their predictive accuracy. If certain parameters are particularly sensitive to these disturbances, they may contribute disproportionately to trajectory errors, making it essential to determine which parameters are most affected by these disturbances. Identifying and quantifying these variations is critical to improving model accuracy, enabling more resilient and adaptive ship control strategies.

This paper examines the impact of external disturbances on the estimation of hydrodynamic parameters in the Abkowitz model and assesses how these variations affect trajectory prediction. By analyzing parameter estimates under different disturbance conditions, this study identifies which parameters are more sensitive to those disturbances and also their impact on maneuvering accuracy. This analysis lays the groundwork for refining ship maneuvering models, improving trajectory prediction under real-world conditions, and guiding the development of disturbance-resilient vessel control strategies.

The remaining of this paper is organized as follows: Section 2 reviews mathematical models for vessel motion, parameter estimation methods, and previous research on the effects of external disturbances. Section 3 explains the methodology, including the Abkowitz model, parameter estimation using least squares, and Sobol sensitivity analysis to identify key parameters affecting prediction errors. Section 4 describes the experimental setup, data collection under different conditions, and presents the sensitivity and variance analysis results. Finally, Section 5 summarizes the main findings of this work and discusses their implications for ship modeling and control.

2 Related Work

Accurate ship maneuvering models are essential for ensuring maritime safety, optimizing vessel performance, and advancing control system design. Over the years, researchers have developed a variety of models, each balancing complexity with data availability. These models include different degrees of freedom and focus on various aspects of ship maneuverability.

Detailed models like the MMG model decompose hydrodynamic forces into contributions from the hull, propeller, and rudder, offering physical insights into ship dynamics Ogawa and Kasai (1978). However, these models require the knowledge of vessel-specific data (such as propeller diameter, rudder area, and rudder aspect ratio), which is not always available Zhang et al. (2023).

In contrast, the Abkowitz model represents the ship as a whole by approximating hydrodynamic forces and moments using polynomial functions of the motion variables Abkowitz (1964). This holistic approach makes the Abkowitz model particularly attractive when only maneuvering data is accessible. In our study, the choice of the Abkowitz model is motivated by the practical constraints of data availability, as it eliminates the need for detailed geometric and propulsive characteristics required by more complex models.

Parameter identification for ship maneuvering models has been addressed by a range of methodologies. Traditional experimental approaches, such as captive model tests, provide controlled environments for estimating hydrodynamic derivatives, as demonstrated in Perera et al. (2015, 2016); Obreja et al. (2010). Meanwhile, high-fidelity numerical methods like Computational Fluid Dynamics (CFD) have been employed to capture complex fluid-structure interactions Liu et al. (2019); Yang et al. (2023). Despite their accuracy, these methods are often resource-intensive and require precise models of the vessel.

In recent years, data-driven approaches have gained popularity. Techniques such as least squares regression Li et al. (2023), maximum likelihood estimation Åström and Källström (1976), extended Kalman filtering Perera et al. (2015, 2016), and Support Vector Machine (SVM) Wang et al. (2021); Luo and Zou (2009); Zhu et al. (2022); Luo and Li (2017) have been successfully applied to estimate the parameters of ship maneuvering models. These methods offer significant advantages, including the ability to model complex, nonlinear relationships without requiring detailed physical models. They are highly adaptable and can improve with more data, making them particularly useful for systems with dynamic or poorly understood behavior. However, they are dependent on the quality of the available data, and inaccurate or sparse data can degrade model performance. Additionally, these approaches can lack interpretability, which can limit understanding of the underlying physical dynamics. In our work, least squares regression was chosen for its balance between computational efficiency and estimation accuracy, particularly when the data is reliable.

Traditionally, many studies have assumed calm water conditions when estimating the vessel parameters, thereby neglecting the impact of disturbances such as wind, waves, and currents Xu and Soares (2025). How-

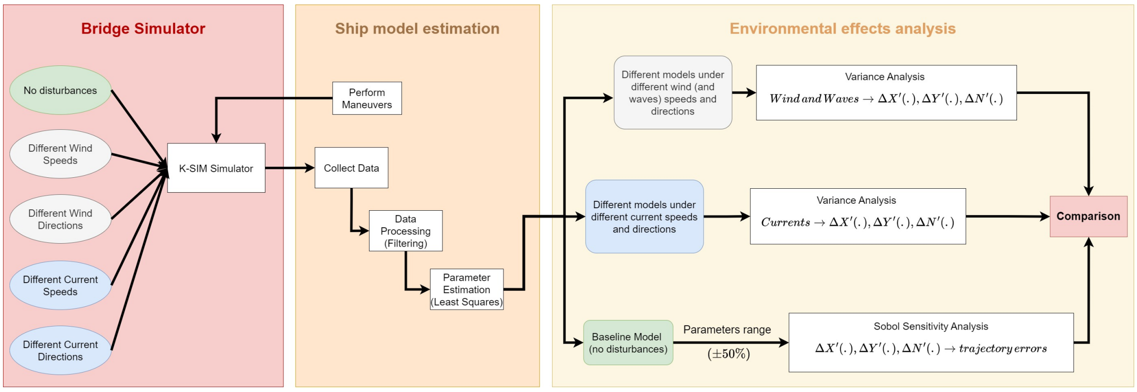

Figure 1: Flowchart of the parameter estimation process and the methodology used in this work.

ever, in real-world conditions, environmental disturbances are always present and can significantly influence ship dynamics. Some recent studies have performed parameter estimation under the influence of disturbances, such as those presented in Wang et al. (2021); Zhu et al. (2022); Xue et al. (2020); Chen et al. (2022). However, in these studies, the disturbances were modeled as stochastic processes represented by Gaussian white noise. By representing disturbances solely as stochastic processes, these studies may not fully account for the structured influence of external conditions on parameter estimation. As a result, the estimated models may lack robustness when applied to real-world scenarios where disturbances follow more complex patterns. Other studies have performed free-running model tests and sea trials in environments where disturbances are inherently present, such as those in Xu et al. (2020); Costa et al. (2021); Xu et al. (2024). However, these works do not provide quantitative assessments of the actual disturbances encountered or their specific impact on the parameter estimation process.

Despite these advances, the literature lacks a detailed analysis of how specific disturbance components contribute to errors in parameter estimation. The work presented in this paper addresses this gap by using data from a high-fidelity bridge simulator to analyze how the hydrodynamic derivatives of the Abkowitz model vary under realistic environmental conditions. Through this approach, it becomes possible to identify which parameters are most sensitive to specific disturbances, offering valuable insights for improving model robustness in real-world applications.

3 Methodology

3.1 Overview of the Estimation Process

The objective of this paper is to analyze the impact of environmental disturbances on the estimation process of the model of the vessel, as illustrated in Figure 1. To achieve this, a baseline model is first estimated under calm conditions by collecting maneuvering data and determining the model's parameters. Subsequently, data is gathered under varying environmental conditions, such as different wind, wave, and current intensities, and a new model is estimated for each case. By comparing parameter variations across different conditions, the influence of disturbances on the estimation process can be assessed. However, analyzing parameter variations alone does not provide insight into prediction errors. A parameter that fluctuates significantly due to environmental effects is not necessarily the primary contributor to prediction inaccuracies. To address this, a Sobol sensitivity analysis is conducted to determine which parameter variations have the greatest impact on prediction errors. By combining both analyses, a more comprehensive understanding of how environmental disturbances affect the accuracy of maneuvering model estimation can be achieved.

This section is organized as follows: Section 3.2 presents the mathematical model used to describe the vessel's motion, Section 3.3 details the parameter estimation method, and Section 3.4 explains the sensitivity analysis methodology.

3.2 Mathematical Model of the Vessel

In this section the Abkowitz 3 DOF model used to describe the motion of the vessel is detailed.

The motion of the vessel, in 3 DOF, can be represented by the position and heading of the vessel $\eta = [x, y, \psi]$, and by the linear and angular velocities (surge, sway and yaw rate) $\nu = [u, v, r]$.

The kinematic model of the vessel can be expressed by equation 1, where $\boldsymbol{R}(\psi)$ represents the rotation matrix around the z axis.

$$\dot{\boldsymbol{\eta}} = \boldsymbol{R}(\psi)\boldsymbol{\nu} \tag{1}$$

Additionally, the kinetic model can be derived from Newton's second law applied to the vessel, resulting in equation 2 where m represents the mass of the vessel, x_g represents the distance from the midships waterline point and the center of gravity point in the x direction, I_z is the moment of inertia around the z-axis, and τ_{RB} represents the total forces on the rigid body of the vessel.

$$\begin{bmatrix} m & 0 & 0 \\ 0 & m & mx_G \\ 0 & mx_G & I_z \end{bmatrix} \begin{bmatrix} \dot{u} \\ \dot{v} \\ \dot{r} \end{bmatrix} + \begin{bmatrix} 0 & -mr & -mx_G r \\ mr & 0 & 0 \\ mx_G r & 0 & 0 \end{bmatrix} \begin{bmatrix} u \\ v \\ r \end{bmatrix} = \tau_{RB} \tag{2}$$

This equation can be rewritten as shown in equation 3, where M_{RB} and C_{RB} represent the rigid body inertia matrix and rigid body Coriolis and centripetal forces matrix, respectively Fossen (2011). The total force τ_{RB} is composed of the control and propulsion forces $\tau_{control}$, the hydrodynamic forces τ_{hyd} (which include added mass, potential damping due to wave radiation, and viscous damping), the hydrostatic forces τ_{hs}, and the environment forces (due to wind, waves and currents) τ_{env}.

$$M_{RB}\dot{\nu} + C_{RB}(\nu)\nu = \tau_{control} + \tau_{hyd} + \tau_{hs} + \tau_{env} \tag{3}$$

Since this study focuses on vessel motion in the horizontal plane (maneuvering theory) without considering roll dynamics, the hydrostatic forces are considered negligible Fossen (2011). Assuming a constant irrotational current ν_c, with $\dot{\nu_c} \approx 0$, the hydrodynamic forces can be expressed by equation 4, where $\nu_r = \nu - \nu_c$ represents the relative velocity of the vessel with respect to the ocean current. Here, M_A represents the added mass matrix due to the inertia of the surrounding fluid, $C_A(\nu_r)$ represents the Coriolis and centripetal matrix, and $D(\nu_r)$ is the hydrodynamic damping matrix. Typically, $C_A(\nu_r)$ and $D(\nu_r)$ are combined as $N(\nu_r) := C_A(\nu_r) + D(\nu_r)$, since distinguishing between the two is difficult in practice Fossen (2011).

$$\tau_{hyd} = -M_A\dot{\nu} - C_A(\nu_r)\nu_r - D(\nu_r)\nu_r \tag{4}$$

$$M_A = \begin{bmatrix} -X_{\dot{u}} & 0 & 0 \\ 0 & -Y_{\dot{v}} & -Y_{\dot{r}} \\ 0 & -N_{\dot{v}} & -N_{\dot{r}} \end{bmatrix} \tag{5}$$

The non-dimensional form of equation 3 is used, as shown in equation 6, since many hydrodynamic derivatives are obtained from model tests Abkowitz (1964). The transformation to non-dimensional parameters is given by equation 8, where ρ is the water density, U is the absolute velocity, and L is the ship length.

$$\begin{bmatrix} m' - X'_{\dot{u}} & 0 & 0 \\ 0 & m' - Y'_{\dot{v}} & m'x'_G - Y'_{\dot{r}} \\ 0 & m'x'_G - N'_{\dot{v}} & I'_z - N'_{\dot{r}} \end{bmatrix} \begin{bmatrix} \dot{u}' \\ \dot{v}' \\ \dot{r}' \end{bmatrix} = \begin{bmatrix} X' \\ Y' \\ N' \end{bmatrix} + \tau'_{wind} \tag{6}$$

In equation 6, $\tau = [X', Y', N']^T$ is a function of u', v', r' and δ, where δ denotes the rudder angle. In the Abkowitz model, the forces τ are expressed as a third-order truncated Taylor series expansion around an initial condition of equilibrium of motion (straight forward motion with constant speed U_0). As discussed in Abkowitz (1964), the Taylor series expansion can yield a large number of parameters to estimate, which is not practical for estimation. Therefore, several assumptions are made to reduce the number of parameters used in the model. These assumption include considering only first-order accelerations, standard port/starboard symmetry, and neglecting coupling terms between the acceleration and velocity. Based on that, τ is expressed by equation 7, where $X'_{(.)}$, $Y'_{(.)}$ and $N_{(.)}'$ represent the partial derivaties of the Taylor series expansion on the equilibrium state, and are refered to as the hydrodynamic derivatives. These derivatives are the parameters to be estimated.

$$\begin{aligned} X' =& X'_u\Delta u' + X'_{uu}\Delta u'^2 + X'_{uuu}\Delta u'^3 + X'_{vv}v'^2 + \\ & X'_{rr}r'^2 + X'_{rv}r'v' + X'_{dd}\delta'^2 + X'_{udd}\Delta u'\delta'^2 + \\ & X'_{vd}v'\delta' + X'_{uvd}\Delta u'v'\delta' \\ Y' =& Y'_v v' + Y'_r r' + Y'_{vvv}v'^3 + Y'_{vvr}v'^2 r' + Y'_{vu}v'\Delta u' \\ & + Y'_{ru}r'\Delta u' + Y'_d\delta' + Y'_{ddd}\delta'^3 + Y'_{ud}\Delta u'\delta' \\ & + Y'_{uud}\Delta u'^2\delta' + Y'_{vdd}v'\delta'^2 + Y'_{vvd}v'^2\delta' + Y'_0 + \\ & Y'_{0u}\Delta u' + Y'_{0uu}\Delta u'^2 \\ N' =& N'_v v' + N'_r r' + N'_{vvv}v'^3 + N'_{vvr}v'^2 r' + N'_{vu}v'\Delta u' \\ & + N'_{ru}r'\Delta u' + N'_d\delta' + N'_{ddd}\delta'^3 + N'_{ud}\Delta u'\delta' \\ & + N'_{uud}\Delta u'^2\delta' + N'_{vdd}v'\delta'^2 + N'_{vv\delta}v'^2\delta' + N_0 + \\ & N'_{0u}\Delta u' + N'_{0uu}\Delta u'^2 \end{aligned} \tag{7}$$

$$\begin{aligned} & m' = \frac{m}{\frac{1}{2}\rho L^3}, \quad x'_G = \frac{x_G}{L}, \quad I'_z = \frac{I_z}{\frac{1}{2}\rho L^5}, \\ & \Delta u' = \frac{\Delta u}{U}, \quad v' = \frac{v}{U}, r' = \frac{Lr}{U}, \quad \delta' = \delta, \\ & \dot{u}' = \frac{\dot{u}}{\left(\frac{U^2}{L}\right)}, \quad \dot{v}' = \frac{\dot{v}}{\left(\frac{U^2}{L}\right)}, \quad \dot{r}' = \frac{\dot{r}}{\left(\frac{U^2}{L}\right)} \\ & X' = \frac{X}{\frac{1}{2}\rho L^2 U^2}, \quad Y' = \frac{Y}{\frac{1}{2}\rho L^2 U^2}, \quad N' = \frac{N}{\frac{1}{2}\rho L^2 U^2} \end{aligned} \tag{8}$$

The non-dimensional hydrodynamic derivatives $X'_{(.)}$,

$Y'_{(.)}$, $N'_{(.)}$ in equation 7 are the parameters that will be estimated for the vessel in Section 4.

The non-dimensional added mass coefficients can be estimated using empirical formulations, Clarke et al. (1982) and Söding (1982) as:

$$\begin{aligned}
Y'_{\dot{v}} &= -\pi\left(\frac{T}{L}\right)^2 \cdot \left(1+0.16\frac{C_B B}{T} - 5.1\left(\frac{B}{L}\right)^2\right)\\
Y'_{\dot{r}} &= -\pi\left(\frac{T}{L}\right)^2 \cdot \left(0.67\frac{B}{L} - 0.0033\left(\frac{B}{T}\right)^2\right)\\
N'_{\dot{v}} &= -\pi\left(\frac{T}{L}\right)^2 \cdot \left(1.1\frac{B}{L} - 0.041\frac{B}{T}\right)\\
N'_{\dot{r}} &= -\pi\left(\frac{T}{L}\right)^2 \cdot \left(\frac{1}{12} + 0.017\frac{C_B B}{T} - 0.33\frac{B}{L}\right)\\
X'_{\dot{u}} &= -\frac{2.7(\frac{m}{\rho})^{5/3}}{\frac{1}{2}L^5}
\end{aligned} \tag{9}$$

where C_B represents the block coefficient, B represents the beam moulded and T represents the draught of the vessel.

As described in Fossen (2011), the wind force and moment in 3 DOF can be calculated as:

$$\tau_{wind} = \begin{bmatrix} \tau_{wind_X} \\ \tau_{wind_Y} \\ \tau_{wind_N} \end{bmatrix} = \frac{1}{2}\rho_a V_{rw}^2 \begin{bmatrix} C_X(\gamma_w) A_{Fw} \\ C_Y(\gamma_w) A_{Lw} \\ C_N(\gamma_w) A_{Lw} L_{oa} \end{bmatrix} \tag{10}$$

where $C_{(.)}$ are the wind coefficients, ρ_a is the air density (1.204 kg/m^3 for 20°C), A_{Fw} is the frontal projected area, A_{Lw} is the lateral projected area, and L_{oa} is the vessel overall length. V_{rw} is the relative wind speed which can be calculated using equation 11, and the wind angle of attack γ_w can be calculated using equation 12.

$$V_{rw} = \sqrt{u_{rw}^2 + v_{rw}^2} = \sqrt{(u-u_w)^2 + (v-v_w)^2} \tag{11}$$

$$\gamma_w = -\operatorname{atan2}(v_{rw}, u_{rw}) \tag{12}$$

The wind speed V_w has a component in the x direction (u_w) and in the y direction (v_w), which can be calculated using equations 13.

$$\begin{aligned} u_w &= V_w \cos(\beta_w - \psi) \\ v_w &= V_w \sin(\beta_w - \psi) \end{aligned} \tag{13}$$

Figure 2 shows the wind vector V_w, the wind direction angle β_w, and wind angle of attack γ_w.

The wind coefficients are calculated, according to

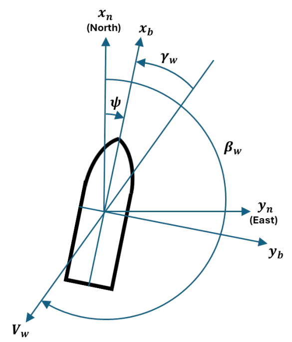

Figure 2: Representation of the wind speed vector V_w and wind direction angle β_w and angle of attack γ_w (based on Fossen (2011)). The figure shows two reference frames: the inertial frame $n = (x_n, y_n)$, where x_n points North and y_n points East, and the body-fixed frame $b = (x_b, y_b)$, which is fixed to the ship, with x_b pointing forward and y_b pointing starboard.

Blendermann (1994), as:

$$\begin{aligned}
C_X(\gamma_w) &= -CD_l \frac{A_{Lw}}{A_{Fw}} \frac{\cos(\gamma_w)}{1 - \frac{\delta_w}{2}\left(1 - \frac{CD_l}{CD_t}\right)\sin^2(2\gamma_w)}\\
C_Y(\gamma_w) &= CD_t \frac{\sin(\gamma_w)}{1 - \frac{\delta_w}{2}\left(1 - \frac{CD_l}{CD_t}\right)\sin^2(2\gamma_w)}\\
C_N(\gamma_w) &= \left[\frac{s_L}{L_{OA}} - 0.18\left(\gamma_w - \frac{\pi}{2}\right)\right] C_Y(\gamma_w)
\end{aligned} \tag{14}$$

where CD_l is the longitudinal resistance, CD_t is the transverse resistance, δ_w is the cross-force, s_L is the horizontal distance from amidships section to center of lateral projected area, and ρ_a is the air density.

The forces generated by waves and currents are not explicitly modeled since these disturbances cannot be directly measured on most vessels. However, their influence will affect the estimation of the Abkowitz hydrodynamic derivatives.

3.3 Parameter Estimation Method

To estimate the hydrodynamic derivatives of the Abkowitz model, described in Section 3.2, several methods can be used, as mentioned in Section 2. In this work Least Square regression is applied since equation 8 can be written in a linear form in terms of the unknown hydrodynamic derivatives.

Considering a dataset with m observations and a linear system of equations given by equation 15:

$$\mathbf{z} = \mathbf{H}\mathbf{x} + \mathbf{w} \tag{15}$$

where $\mathbf{x}$ is an $n \times 1$ column vector of unknowns, $\mathbf{z}$ is an $m \times 1$ column vector of observed values, $\mathbf{H}$ is an $m \times n$ matrix of coefficients, and $\mathbf{w}$ is an $m \times 1$ column vector representing the noise in the system.

The goal of the least squares method is to find the vector $\mathbf{x}$ that minimizes the sum of the squares of the differences between the observed values $\mathbf{z}$ and the predicted values $\mathbf{Hx}$.

As described in Bar-Shalom et al. (2001), this method can be expressed as minimizing the objective function $J(x)$, as expressed in equation 16.

$$J(x) = ||\mathbf{z} - \mathbf{Hx}||^2 \tag{16}$$

The solution to minimizing the objective function $J(x)$ can be calculated by equation 17.

$$\hat{x} = \arg\min_{\mathbf{x}} J(x) = (\mathbf{H}^T\mathbf{H})^{-1}\mathbf{H}^T\mathbf{z} \tag{17}$$

It is important to note that the least square solution only exists if there are enough independent observations in the data. This condition implies that there must be at least n linearly independent observations in the dataset, where n is the number of parameters to be estimated.

The discretization of equations 6 using Euler's stepping method results in equation 18, where $m_{11} = m' - X'_{\dot{u}}, m_{22} = m' - Y'_{\dot{v}}, m_{23} = m'x'_G - Y'_{\dot{r}}, m_{32} = m'x'_G - N'_{\dot{v}}$, and $m_{33} = I'_z - N'_{\dot{r}}$.

$$\begin{aligned}
&m_{11}(\frac{u(k+1)-u(k)}{\Delta t})L = U^2X' + U^2\tau'_X\\
&m_{22}(\frac{v(k+1)-v(k)}{\Delta t})L + m_{23}(\frac{r(k+1)-r(k)}{\Delta t})L^2 = U^2Y' + U^2\tau'_Y\\
&m_{32}(\frac{v(k+1)-v(k)}{\Delta t})L + m_{33}(\frac{r(k+1)-r(k)}{\Delta t})L^2 = U^2N' + U^2\tau'_N
\end{aligned} \tag{18}$$

Additionally, X', Y', and N', from equation 7 can be rewritten as:

$$\begin{aligned}
U^2X' &= Ax\\
U^2Y' &= By\\
U^2N' &= C
\end{aligned} \tag{19}$$

where

$$\begin{aligned}
A =&[X'_u, X'_{uu}, X'_{uuu}, X'_{vv}, X'_{rr}, X'_{rv}, X'_{dd}, X'_{udd}, X'_{vd}, X'_{uvd}]^T\\
B =&[Y'_v, Y'_r, Y'_{vvv}, Y'_{vvr}, Y'_{vu}, Y'_{ru}, Y'_d, Y'_{ddd}, Y'_{ud}, Y'_{uud}, Y'_{vdd}, Y'_{vvd},\\
&Y'_0, Y'_{0u}, Y'_{0uu}]^T\\
C =&[N'_v, N'_r, N'_{vvv}, N'_{vvr}, N'_{vu}, N'_{ru}, N'_d, N'_{ddd}, N'_{ud}, N'_{uud},\\
&N'_{vdd}, N'_{vv\delta}, N_0, N'_{0u}, N'_{0uu}]^T\\
x =&[U\Delta u, \Delta u^2, \frac{\Delta u^3}{U}, v^2, L^2r^2, rvL, U^2\delta^2, U\Delta u\delta^2, Uv\delta, \Delta uv\delta]\\
y =&[Uv, UrL, \frac{v^3}{U}, \frac{v^2rL}{U}, v\Delta u, rL\Delta u, U^2\delta, U^2\delta^3, \Delta uU\delta, \Delta u^2\delta,\\
&Uv\delta^2, v^2\delta, U^2, U\Delta u, \Delta u^2]\\
n =&[Uv, UrL, \frac{v^3}{U}, \frac{v^2rL}{U}, v\Delta u, rL\Delta u, U^2\delta, U^2\delta^3, \Delta uU\delta, \Delta u^2\delta,\\
&Uv\delta^2, v^2\delta, U^2,\\
&U\Delta u, \Delta u^2]
\end{aligned} \tag{20}$$

The vectors A, B, and C are the 40 hydrodynamic derivatives to be estimated using the least square method.

3.4 Sobol Sensitivity Analysis

The main objective of this work is to understand how the environmental disturbances affect the estimation of the vessel model. To achieve this, it is necessary to analyze not only how the estimation of the hydrodynamic derivatives varies with the different environmental conditions, but also which hydrodynamic derivative contributes the most to deviations in the predicted trajectory.

To address the last point, Sobol sensitivity analysis is used. This variance-based technique quantifies the contribution of each input parameter to the overall variability in the model's predictions, thereby identifying the most influential parameters. By decomposing the output variance into contributions from individual parameters and their interactions, Sobol sensitivity analysis provides a comprehensive assessment of parameter importance.

The first-order Sobol index S_i quantifies the direct contribution of each input parameter to the output variance. In contrast, the total-order Sobol index S_{T_i} accounts for both the direct effects and all interactions involving the parameters X_i. Equation 21 defines the total-order index, where $X_{\sim i}$ represents all parameters except X_i, $V(Y)$ represents the total variance of the output, and $\mathrm{E}_{X_{\sim i}}[\mathrm{V}_{X_i}(Y|X_{\sim i})]$ represents the expected value of the conditional variance of Y given all input parameters except X_i. More details about this method can be found in Sobol (2001).

$$S_{T_i} = \frac{E_{X_{\sim i}}\left[V_{X_i}(Y|X_{\sim i})\right]}{V(Y)} \tag{21}$$

In this study, only the total-order indices S_{T_i} are considered, as they provide a more comprehensive measure of parameter importance.

The analysis consists of analyzing the impact of the 40 hydrodynamic derivatives of the Abkowitz model (vectors A, B and C in equation 20) on the prediction error of the model. Therefore, each parameter is varied within a range of $\pm 50\%$ of its baseline value, which was initially estimated under no external disturbances (Section 4.2). Subsequently, for each generated set of parameter values, the mean distance error between the predicted and reference trajectories is used as a metric to evaluate model accuracy and quantify the sensitivity of the error with respect to each parameter.

By conducting this analysis, the most critical hydrodynamic derivatives influencing the accuracy of the Abkowitz model can be identified.

4 Experimental Results

4.1 Experimental Setup

In order to estimate the maneuvering model of the vessel, data from different maneuvers must be collected. For this purpose, a professional navigation bridge simulator, the K-sim Navigation, manufactured by Kongsberg Maritime AS, is used, as shown in Figure 3. This simulator is highly accurate and realistic, commonly used for training nautical students and professional captains. It allows for a wide range of environmental conditions to be simulated, and for the collection of detailed maneuvering data.

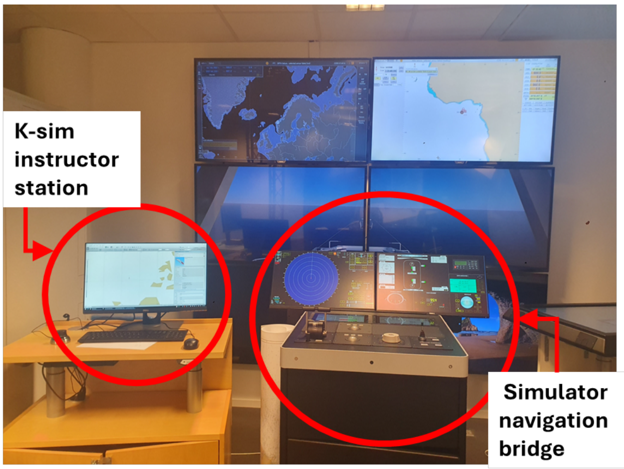

Figure 3: K-sim Kongsberg simulator.

The K-Sim simulator includes various vessel types, and for this study, a Ro-Ro ferry (Ferry Basto Fosen IV) is used. The vessel's characteristics are detailed in Table 1. This vessel is equipped with two azimuth thrusters, one at the bow and one at the stern. Although the mathematical model described in the previous chapter uses the rudder angle as the control variable, it is assumed that adjusting the azimuth thruster angle has an equivalent effect, in terms of model structure, to changing the rudder angle in a rudder-propeller configuration. In the performed maneuvers the rudder angle was varied in the range of $-35°$ to $35°$.

During the maneuvers, the azimuth thrusters operate at a constant speed of 206 rpm, while the propeller pitch is maintained at 80% of the nominal pitch setting. During the maneuvers, only the angle of the thruster is adjusted. Additionally, the vessel's nominal speed, U_0, was found to be 10.51 knots.

An important aspect highlighted in Wang and Zou (2018) is that using a single maneuver in the dataset for the estimation of the model can increase the dataset collinearity, which may lead to inaccurate estimations. Additionally, relying on just one maneuver makes it

Table 1: Characteristics of FERRY62 ship.

Variable	Description	Value
L_{pp}	Length between perpendicular	137.2 m
L_{OA}	Length overall	142.9 m
B	Beam moulded	21 m
T_a	Draught aft	4.5 m
T_{fwd}	Draught fore	4.5 m
m	Displacement	4726 ton
C_B	Block coefficient	0.36
k_z	Radius of inertia (multiples of L_{pp})	0.26
A_{L_w}	Lateral windage area	1400 m^2

challenging to accurately predict maneuvers with different rudder angles. To avoid this, it is beneficial to include a variety of maneuvers with different rudder angles in the dataset, ensuring that a wider range of the vessel's dynamics is captured. For that reason, in this work, the maneuvers performed to collect the data for the model estimation included three zigzag maneuvers (zigzag 10/10, zigzag 20/20, and zigzag 30/30) and one random maneuver (with rudder variation from -35° to 35°). Additional maneuvers were conducted for model validation. All maneuvers were performed over 20 minute period with a frequency of 2 Hz. The collected variables include:

- Surge speed (knots)
- Sway speed (knots)
- Yaw rate (°/min)
- Latitude and longitude (radians)
- Heading (°)
- Wind direction (°)
- Wind speed (knots)

To evaluate the influence of environmental conditions, four variables were controlled: wind direction, wind speed, current direction, and current speed. These variables were kept constant throughout each maneuver, meaning wind gusts were not considered. Additionally, when wind was introduced into the simulation, waves were generated accordingly. However, wave and current data were not collected from the simulator, as most vessels lack the means to measure them. Consequently, these forces were not explicitly modeled in equation 6. Nevertheless, they may still impact the model's accuracy.

Despite the absence of measurement noise in the simulator data, filtering is still necessary, especially in high-disturbance conditions. Since the ferry in the K-Sim simulator has six degrees of freedom, motion in one direction can influence movement in another due

Table 2: Estimated hydrodynamic derivatives for the Ro-Ro Ferry Basto Fosen IV under no wind scenario.

Parameters in surge		Parameters in sway		Parameters in yaw	
Xu	-1.311×10^{-3}	Yv	-9.386×10^{-3}	Nv	-9.057×10^{-4}
Xuu	-5.536×10^{-4}	Yr	-4.438×10^{-3}	Nr	-5.603×10^{-4}
Xuuu	-8.713×10^{-4}	Yvvv	-1.289×10^{-1}	Nvvv	-1.748×10^{-2}
Xvv	1.070×10^{-2}	Yvvr	-8.920×10^{-2}	Nvvr	-1.300×10^{-2}
Xrr	-5.975×10^{-3}	Yvu	-4.587×10^{-3}	Nvu	-9.204×10^{-4}
Xrv	-6.460×10^{-3}	Yru	-3.919×10^{-3}	Nru	-3.360×10^{-4}
Xdd	-1.090×10^{-3}	Yd	-1.223×10^{-4}	Nd	-5.045×10^{-5}
Xudd	3.537×10^{-3}	Yddd	2.450×10^{-4}	Nddd	9.983×10^{-5}
Xvd	1.575×10^{-3}	Yud	-1.061×10^{-5}	Nud	2.246×10^{-4}
Xuvd	4.982×10^{-3}	Yuud	-1.529×10^{-3}	Nuud	-2.260×10^{-4}
		Yvdd	-1.243×10^{-2}	Nvdd	-2.016×10^{-3}
		Yvvd	7.860×10^{-2}	Nvvd	8.757×10^{-3}
		Y0	1.111×10^{-6}	N0	2.043×10^{-7}
		Y0u	4.908×10^{-5}	N0u	9.482×10^{-6}
		Y0uu	6.966×10^{-5}	N0uu	1.395×10^{-5}

to hydrodynamic coupling. For example, rolling motion can introduce oscillations in sway speed. These oscillations must be filtered before estimating the parameters of the 3-DOF model in equation 6. Therefore, a 5th-order Butterworth low-pass filter with a cutoff frequency of 0.04 Hz was applied to the surge speed, sway speed, and yaw rate data to attenuate these oscillations.

To validate the estimated model, the predicted trajectories of the model are compared to the actual trajectory obtained from the simulator. Different maneuvers from those used to estimate the model are used for the validation. The mean distance error (MDE) is used as the evaluation metric, defined as:

$$MDE = \frac{1}{N}\sum_{i=1}^{N}\sqrt{(x_i - \hat{x}_i)^2 + (y_i - \hat{y}_i)^2} \tag{22}$$

where x_i and y_i are the actual positions from the simulator data, and $\hat{x}_i$ and $\hat{y}_i$ are the predicted positions from the model.

4.2 Model Estimation Under No Disturbances

In this section, the hydrodynamic derivatives of the ship maneuvering model are estimated under no external disturbances. Using the four estimation maneuvers mentioned in Section 4.1, the estimated hydrodynamic derivatives are presented in Table 2. These values serve as baseline parameters for comparison with those estimated under environmental disturbances in subsequent sections.

To assess the accuracy of the estimated model, its predictions are compared against simulator data for maneuvers not used in parameter estimation. The validation maneuvers include a zigzag 15/15 and a turning 20 maneuver. Figure 4 presents the predicted ship trajectories (on the left) and the corresponding surge speed, sway speed, and yaw rate (on the right). The comparison shows the agreement between the model predictions and the actual simulator data, demonstrating the model's capability to capture vessel dynamics when there is no disturbance.

The model's accuracy is further assessed using mean distance error (MDE) and maximum distance error, as shown in Table 3. The results indicate that despite small accumulations over a 20-minute period, the errors remain within an acceptable range given the vessel's size.

Table 3: Results of the performance of the estimated model in different maneuvers.

Maneuver	Mean distance error [m]	Maximum distance error [m]
Zigzag 10/10	71.898	154.157
Zigzag 20/20	52.480	190.421
Zigzag 30/30	99.925	178.161
Random	67.160	115.649
Zigzag 15/15	71.219	172.912
Turning 20	56.812	89.923

4.3 Impact of Wind Disturbances on Parameters Estimation

This section analyzes the impact of wind disturbances in the estimation of the hydrodynamic derivatives of the model, and therefore no currents are considered in this section. The same four maneuvers are collected in different wind speeds and wind directions, generating different models for each condition. Then the corre-

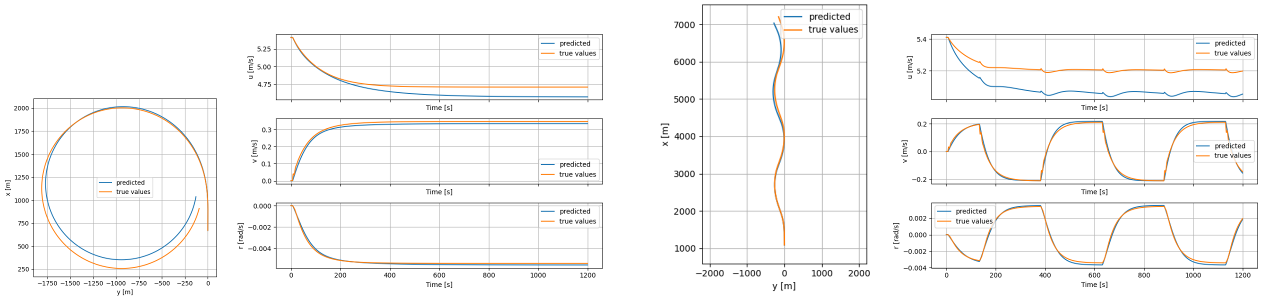

(a) Turning maneuver. (b) Zigzag 15/15

Figure 4: Validation of the estimated model under no environmental disturbances.

sponding hydrodynamic derivatives of each model were compared.

To analyze the impact of different wind speeds (and corresponding waves) on the estimation process, five models were estimated under different wind speeds (2 knots, 7 knots, 12 knots, 17 knots, and 22 knots). The wind direction was kept constant at 45 degrees. The values of the hydrodynamic derivative of each of these models, as well as the mean value and the variance, are shown in Figure 5. As wind speed increases, the presence of unmodeled disturbances also grows, leading to deviations in parameter estimation. This is expected, as stronger wind conditions introduce additional forces and moments that are not explicitly accounted for in the baseline model.

The results of the analysis of the variance of the parameters reveal that in the surge force equation (X), the parameters Xrv, Xvv, and Xrr show the highest variation. In Y, the parameters showing the highest variation are Yvvv, Yvvr, and Yvvd. A similar trend is seen in N, where the parameters with the highest variation are the same as in the sway force Y.

The effect of varying wind direction, while maintaining a constant wind speed, is analyzed next. Similar to the previous analysis, different models are estimated using data collected from the four estimation maneuvers performed at different angles of attack. Five models were estimated with wind speeds of 12 knots at directions of 0°, 45°, 90°, 135°, and 180°. Figure 6 shows the parameter values of the different models as well as the mean and variance. From this figure similar observation to the wind speed effects can be taken. In all X, Y and N the parameters with the highest variations are the same as when the wind speed was varied.

4.4 Impact of Currents on Parameter Estimation

In a similar approach as the previous section, the effect of current disturbances on the estimation of the hydrodynamic derivatives of the model is now analyzed.

The same four maneuvers were used for the estimation of the models, however this time they were collected under different current speeds and directions, with no wind disturbances. Separate models were then estimated for each condition, and the hydrodynamic derivatives were compared.

Focusing only on changes on the current speed, four models were estimated with currents at 45° and speeds of 1 knot, 3 knots, 5 knots, and 7 knots. The variation in the hydrodynamic parameters is shown in Figure 7.

Compared to wind disturbances, a larger number of hydrodynamic derivatives exhibit significant variation under changing current conditions. In X, the parameters showing higher variation are Xrv, Xudd, Xuuu, Xvv, and Xuu. In Y, significant variation is observed in Yvvv, Yvvr, Yvu, Yvvd, Yru, Y0uu, and Y0u. Similarly, in N, higher variations occur in Nvvv, Nvu, Nvvr, Nvvd, N0uu, N0u, Nru, and Nv.

The second part of the analysis evaluates the effect of changing current direction while maintaining a constant speed. As in the previous case, five models were estimated with a current speed of 3 knots at directions of 0°, 45°, 90°, 135°, and 180°. The variation in the hydrodynamic parameters is illustrated in Figure 8.

In X, parameters such as Xuuu, Xrr, Xudd, Xuvd, Xrv, Xvv, Xuu show significant variation. In Y, the parameters Yvvr, Yvvv, Yv, Yvvd show high variation, while Yvu, Yvdd, Yuud, Y0u, Yr, Yddd, and Y0 also vary considerably, though to a lesser extent. A similar trend is observed in N, where Nvvr, Nvvv, Nvvd, Nv, and Nvdd exhibit substantial variation, whereas Nvu, Nr, N0u, Nuud, Nddd, N0, Nud, and N0uu, show smaller fluctuations.

The two analyses (Sections 4.3 and 4.4) provide insight into how external disturbances affect the estimation of model parameters, identifying which parameters are most susceptible to variation under wind and current disturbances. However, the parameters that fluctuate the most are not necessarily the primary contrib-

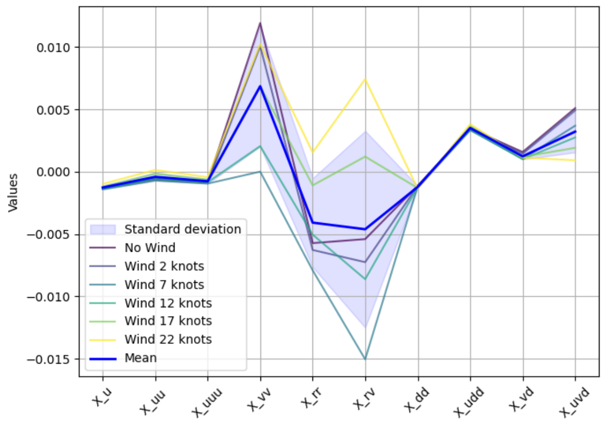

(a)

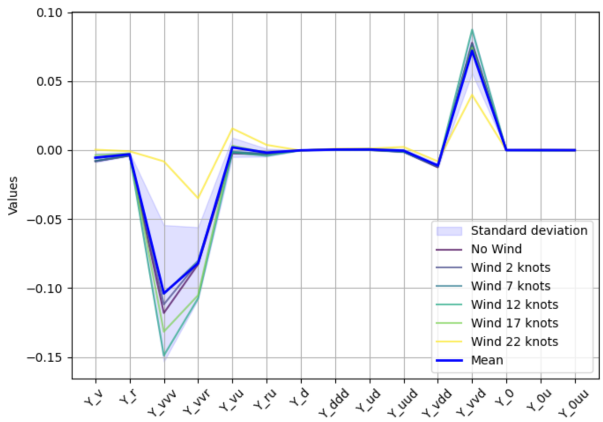

(b)

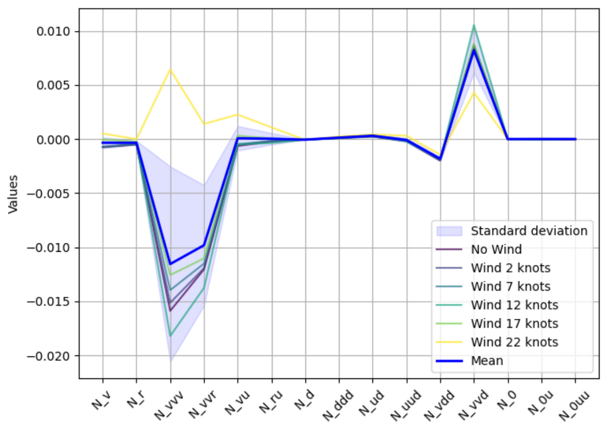

(c)

Figure 5: Impact of different current speeds in the $X'(.)$,$Y'(.)$, and $N'(.)$ parameters.

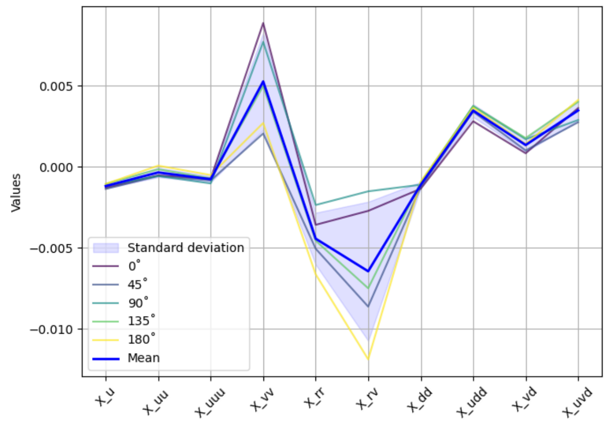

(a)

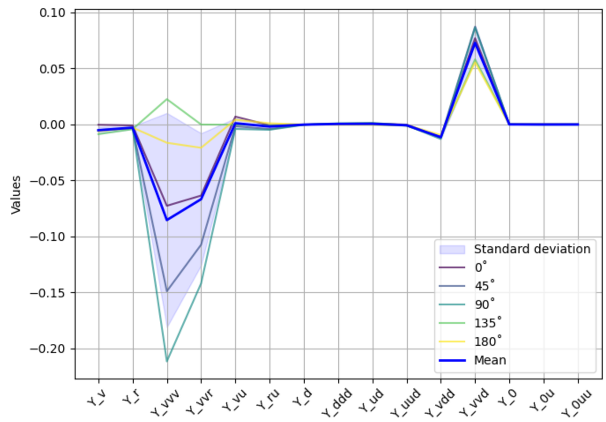

(b)

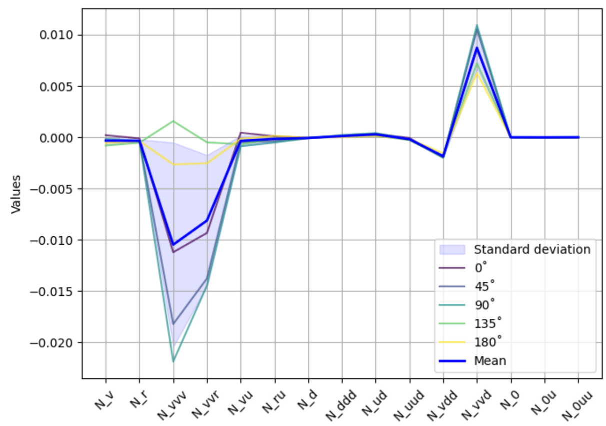

(c)

Figure 6: Impact of different current directions in the $X'(.)$,$Y'(.)$, and $N'(.)$ parameters.

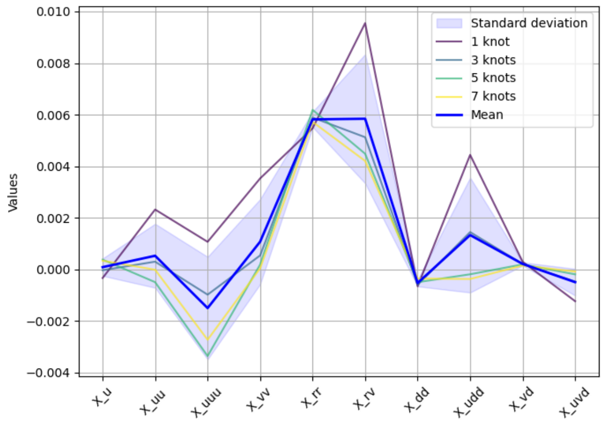

(a)

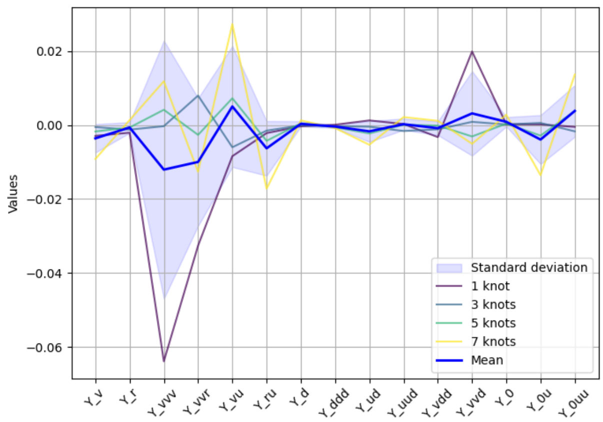

(b)

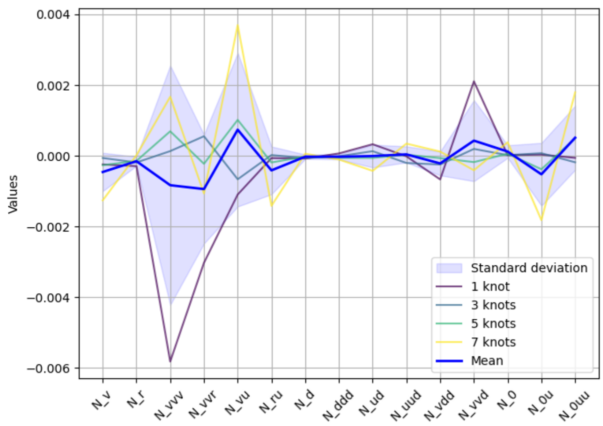

(c)

Figure 7: Impact of different current speeds in the $X'(.)$,$Y'(.)$, and $N'(.)$ parameters.

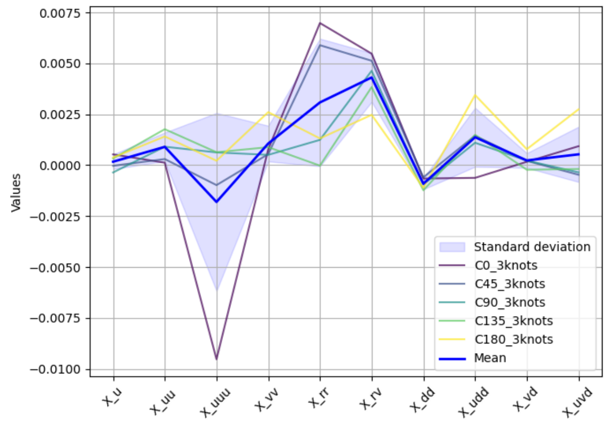

(a)

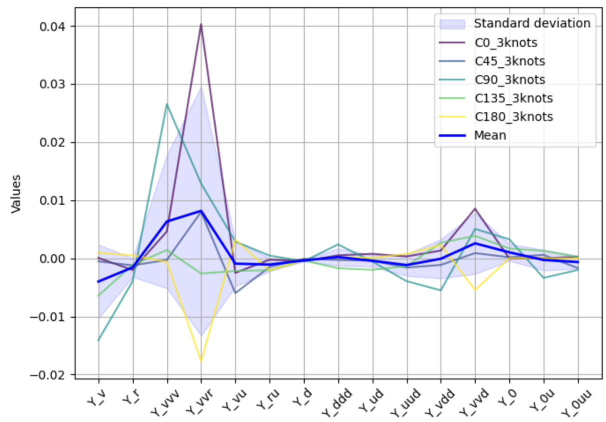

(b)

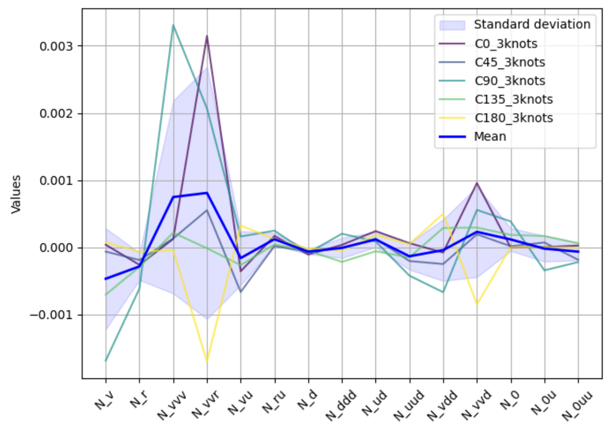

(c)

Figure 8: Impact of different current directions in the $X'(.)$,$Y'(.)$, and $N'(.)$ parameters.

Table 4: Sensitivity analysis results.

Parameter sensitivity in X		Parameter sensitivity in Y		Parameter sensitivity in N	
Xdd	2.523×10^{-5}	Y0	1.394×10^{-3}	N0	9.705×10^{-1}
Xrr	1.387×10^{-6}	Yr	4.062×10^{-5}	Nr	2.050×10^{-2}
Xrv	5.638×10^{-8}	Yv	4.287×10^{-6}	Nv	9.252×10^{-3}
Xvv	2.365×10^{-9}	Yd	4.131×10^{-7}	Nvdd	4.220×10^{-4}
Xu	1.012×10^{-9}	Yvdd	2.812×10^{-7}	Nd	4.080×10^{-4}
Xvd	8.859×10^{-10}	Y0u	2.002×10^{-8}	N0u	4.605×10^{-5}
Xudd	8.868×10^{-11}	Yddd	1.715×10^{-8}	Nddd	2.064×10^{-5}
Xuvd	4.476×10^{-15}	Yru	2.669×10^{-10}	Nvvd	4.723×10^{-7}
Xuu	1.285×10^{-15}	Yvvd	2.405×10^{-10}	Nvvr	3.164×10^{-7}
Xuuu	3.061×10^{-21}	Yvvr	2.062×10^{-10}	Nru	2.929×10^{-7}
		Yvvv	8.141×10^{-11}	Nud	1.015×10^{-7}
		Yvu	1.913×10^{-11}	Nvvv	6.293×10^{-8}
		Yud	3.688×10^{-12}	Nvu	3.635×10^{-8}
		Y0uu	2.550×10^{-14}	N0uu	4.555×10^{-11}
		Yuud	5.569×10^{-18}	Nuud	1.424×10^{-13}

utors to prediction error. To determine which parameter variations have the greatest impact on prediction accuracy, a sensitivity analysis is required.

4.5 Sensitivity Analysis Results

In this paper, the Sobol sensitivity analysis is performed to assess the impact that variations in the hydrodynamic parameters of the Abkowitz model (equation 7) have on the accuracy of predicted trajectories. The parameters are varied within a range of ±50% from their baseline values (the model estimated under no disturbances in Section 4.2), and their influence on the trajectory prediction error is analyzed.

The results of this analysis are presented in Table 4, with the parameters ranked according to their sensitivity. A significant discrepancy is observed between the most sensitive parameter and the others in all force vector components (X, Y, and N). Since Y and N are coupled in equation 18, their relative sensitivity follows a similar order. Additionally, because the sway force Y and the yaw moment N include a bias terms independent of the states u, v, r, and δ (that is, Y0 and N0), these terms exhibit the highest sensitivity by a significant margin.

These findings highlight the parameters whose variations contribute most to trajectory prediction errors. This information can be used to evaluate whether the environmental disturbances lead to variations in highly sensitive parameters, potentially increasing prediction errors.

4.6 Discussion

Comparing the impact of environmental disturbances on the model parameters (Sections 4.3 and 4.4) with the sensitivity analysis (Section 4.5) allows us to determine whether the parameters that vary the most due to the disturbances are also the ones that, when altered, contribute most to the trajectory prediction error.

From the wind impact analysis (Section 4.3), in the X force vector, most parameters that exhibit significant variation due to wind disturbances have low sensitivity values, except for Xrr, which shows the third-largest variation but is also the second-most sensitive parameter according to the Sobol sensitivity analysis. In both the Y force and N moment vectors, the parameters that experience the highest variation due to wind also have low sensitivity values. This suggests that trajectory prediction errors cannot be solely attributed to the parameters most affected by wind disturbances. Instead, errors arise from a combination of parameters that exhibit limited variation but have high sensitivity values, such as Xrr.

Regarding the impact of currents, a greater number of parameters show variations compared to wind disturbances. In the X force vector, Xrr, the second-most sensitive parameter, exhibits only minor variation when current speed increases but undergoes significant changes when the current direction shifts. However, most other parameters with large variations due to current disturbances have low sensitivity values. Similarly, in the Y force and N moment vectors, the parameters that change the most due to currents generally have low sensitivity values. Thus, as with wind disturbances, trajectory prediction errors cannot be explained solely by the parameters that vary the most due to currents. Instead, errors result from a combination of parameters with smaller variations but higher sensitivity values, such as Xrr, Yv, and Nv.

Table 5 summarizes these findings, highlighting the parameters with the greatest variance due to wind and

Table 5: Summary of the disturbance variance analysis and the sensitivity analysis of the hydrodynamic parameters.

	Wind Speed	Wind direction	Current Speed	Current direction	Sensitivity Analisis
X'(.)	**Xrv**, Xvv, **Xrr**	**Xrv**, Xvv, **Xrr**	**Xrv**, Xudd, Xuuu, Xvv, Xuu	Xuuu, **Xrr**, Xudd, Xuvd, **Xrv**, Xvv, Xuu	Xdd, **Xrr**, **Xrv**
Y'(.)	Yvvv, Yvvr, Yvvd	Yvvv, Yvvr, Yvvd	Yvvv, Yvvr, Yvu, Yvvd, Yru, Y0uu, Y0u	Yvvr, Yvvv, Yv, Yvvd	Y0, Yr, **Yv**
N'(.)	Nvvv, Nvvr, Nvvd	Nvvv, Nvvr, Nvvd	Nvvv, Nvu, Nvvr, Nvvd, N0uu, N0u, **Nv**	Nvvr, Nvvv, **Nv**, Nvvd, Nvdd	N0, Nr, **Nv**

current speed and direction changes, as well as the three parameters with the highest sensitivity values. These results emphasize the importance of considering both parameter sensitivity and variance when evaluating the effects of environmental disturbances on model accuracy. Simply identifying the most fluctuating parameters is insufficient; understanding which variations significantly impact prediction errors is crucial for improving model reliability.

5 Conclusion

This study analysed the impact of environmental disturbances, such as wind, waves, and currents, on the estimation of hydrodynamic parameters in the Abkowitz model and their effect on trajectory prediction accuracy.

First, a Sobol sensitivity analysis was conducted to determine which parameters have the greatest influence on trajectory prediction errors. The results revealed that in all three degrees of freedom, there is always one hydrodynamic derivative to which the predictions are particularly sensitive to, exhibiting significantly higher sensitivity values than the others. Additionally, most hydrodynamic derivatives in the moment in yaw demonstrated higher sensitivity compared to those in the surge and sway force equations.

Next, data from multiple maneuvers were collected under different environmental conditions, and models were estimated to analyze parameter variations. The results showed that in most cases, the parameters exhibiting the highest variation were not necessarily the most sensitive ones. However, some parameters with high sensitivity also experienced noticeable variation, indicating a potential link between environmental disturbances and trajectory prediction errors. Furthermore, the presence of currents was found to affect a broader set of parameters compared to wind and wave disturbances.

These findings highlight the importance of considering environmental influences in ship model estimation to improve trajectory prediction reliability. They also emphasize the need for enhanced parameter estimation techniques that are robust to external disturbances. By identifying the most sensitive parameters, this study provides a foundation for refining ship modeling methods and developing compensation strategies to mitigate the effects of environmental variability.

Acknowledgments

The work presented here is supported by the RoboSAPIENS project funded by the European Commission's Horizon Europe programme under grant agreement number 101133807.

References

Abkowitz, M. *Lectures on Ship Hydrodynamics - Steering and Manoeuvrability.* Hydro of Aerodynamisk Laboratorium, 1964.

Bar-Shalom, Y., Li, X. R., and Kirubarajan, T. *Estimation with Applications to Tracking and Navigation.* John Wiley & Sons, 2001.

Blendermann, W. Parameter identification of wind loads on ships. *Journal of Wind Engineering and Industrial Aerodynamics*, 1994. 51(3):339–351. doi:10.1016/0167-6105(94)90067-1.

Chen, L., Yang, P., Li, S., Tian, Y., Liu, G., and Hao, G. Grey-box identification modeling of ship maneuvering motion based on ls-svm. *Ocean Engineering*, 2022. 266:112957. doi:10.1016/j.oceaneng.2022.112957.

Clarke, D., Gedling, P., and G.Hine. The application of manoeuvring criteria in hull design using linear theory. *The Royal Institution of Naval Architects*, 1982.

Costa, A., Xu, H., and Guedes Soares, C. Robust parameter estimation of an empirical manoeuvring model using free-running model tests. *Journal of Marine Science and Engineering*, 2021. 9:1302. doi:10.3390/jmse9111302.

Du, P., Cheng, L., Tang, Z.-j., Ouahsine, A., Hu, H.-b., and Hoarau, Y. Ship maneuvering prediction based on virtual captive model test and system dynamics approaches. *Journal of Hydrodynamics*, 2022. 34. doi:10.1007/s42241-022-0029-0.

Fossen, T. I. *Handbook of Marine Craft Hydrodynamics and Motion Control*. John Wiley & Sons, Ltd., 2011.

Li, S., Wang, T., Li, G., and Zhang, H. Ship maneuvering model optimization for improved identification with less excitation. *Ocean Engineering*, 2023. 280:114540. doi:10.1016/j.oceaneng.2023.114540.

Liu, Y., Zou, L., and Zou, Z. Computational fluid dynamics prediction of hydrodynamic forces on a manoeuvring ship including effects of dynamic sinkage and trim. *Proceedings of the Institution of Mechanical Engineers, Part M: Journal of Engineering for the Maritime Environment*, 2019. 233(1):251–266. doi:10.1177/1475090217734685.

Luo, W. and Li, X. Measures to diminish the parameter drift in the modeling of ship manoeuvring using system identification. *Applied Ocean Research*, 2017. 67:9–20. doi:10.1016/j.apor.2017.06.008.

Luo, W. and Zou, Z. Parametric identification of ship maneuvering models by using support vector machines. *Journal of Ship Research*, 2009. 53:19–30. doi:10.5957/jsr.2009.53.1.19.

Obreja, D., Nabergoj, R., Crudu, L., and Păcuraru-Popoiu, S. Identification of hydrodynamic coefficients for manoeuvring simulation model of a fishing vessel. *Ocean Engineering*, 2010. 37(8):678–687. doi:10.1016/j.oceaneng.2010.01.009.

Ogawa, A. and Kasai, H. On the mathematical model of manoeuvring motion of ships. *International shipbuilding progress*, 1978. 25:306–319.

Perera, L., Oliveira, P., and Soares, C. G. System identification of nonlinear vessel steering. *Journal of Offshore Mechanics and Arctic Engineering*, 2015. 137. doi:10.1115/1.4029826.

Perera, L., Oliveira, P., and Soares, C. G. System identification of vessel steering with unstructured uncertainties by persistent excitation maneuvers. *IEEE Journal of Oceanic Engineering*, 2016. 41:515–527. doi:10.1109/JOE.2015.2460871.

Sobol, I. Global sensitivity indices for nonlinear mathematical models and their monte carlo estimates. *Mathematics and Computers in Simulation*, 2001.

Söding, H. Prediction of ship steering capabilities. 1982. 29:3–29.

Wang, T., Æsøy, V., and Zhang, H. Parameter identification of ship manoeuvring model under disturbance using support vector machine method. *Ships and Offshore Structures*, 2021. 16. doi:10.1080/17445302.2021.1927600.

Wang, Z., Xu, H., Xia, L., Zou, Z., and Soares, C. G. Kernel-based support vector regression for nonparametric modeling of ship maneuvering motion. *Ocean Engineering*, 2020. 216:107994. doi:10.1016/j.oceaneng.2020.107994.

Wang, Z. and Zou, Z. Quantifying Multicollinearity in Ship Manoeuvring Modeling by Variance Inflation Factor. volume Volume 7A: Ocean Engineering of *International Conference on Offshore Mechanics and Arctic Engineering*. 2018. doi:10.1115/OMAE2018-77121.

Xu, H., Silva, P., and Guedes Soares, C. Effect of sampling rate in sea trial tests on the estimation of hydrodynamic parameters for a nonlinear ship manoeuvring model. *Journal of Marine Science and Engineering*, 2024. 12:407. doi:10.3390/jmse12030407.

Xu, H. and Soares, C. G. Review of system identification for manoeuvring modelling of marine surface ships. *Journal of Marine Science and Application*, 2025. doi:10.1007/s11804-025-00681-w.

Xu, P.-F., Cheng, C., Cheng, H.-X., Shen, Y.-L., and Ding, Y.-X. Identification-based 3 dof model of unmanned surface vehicle using support vector machines enhanced by cuckoo search algorithm. *Ocean Engineering*, 2020. 197:106898. doi:10.1016/j.oceaneng.2019.106898.

Xue, Y., Liu, Y., Ji, C., and Xue, G. Hydrodynamic parameter identification for ship manoeuvring mathematical models using a bayesian approach. *Ocean Engineering*, 2020. 195:106612. doi:10.1016/j.oceaneng.2019.106612.

Yang, Y., Chillcce, G., and Moctar, O. Mathematical modeling of shallow water effects on ship maneuvering. *Applied Ocean Research*, 2023. 136:103573. doi:10.1016/j.apor.2023.103573.

Yang, Y. and el Moctar, O. A mathematical model for ships maneuvering in deep and shallow waters. *Ocean Engineering*, 2024. 295:116927. doi:10.1016/j.oceaneng.2024.116927.

Zhang, S., Wu, Q., Liu, J., He, Y., and Li, S. State-of-the-art review and future perspectives on maneuvering modeling for automatic ship berthing. *Journal of Marine Science and Engineering*, 2023. 11. doi:10.3390/jmse11091824.

Zhu, M., Wang, T., Zhang, H., and Li, G. Ship manoeuvring model identification under wind disturbance. In *2022 IEEE International Conference on Real-time Computing and Robotics (RCAR)*. pages 648–653, 2022. doi:10.1109/RCAR54675.2022.9872289.

Åström, K. and Källström, C. Identification of ship steering dynamics. *Automatica*, 1976. 12(1):9–22. doi:10.1016/0005-1098(76)90064-9.